On the predictability of the cutting forces of small, longitudinal cutter heads

Michael Berner[1], **Nikolaus A. Sifferlinger**[2], **Roman Gerer**[3]

[1]Senior Researcher, Department of Mineral Resources Engineering - Conveying Technology and Design Methods, University of Leoben, Austria, e-mail: michael.berner@unileoben.ac.at.

[2]Professor for Excavation Engineering and Conveying Technology and Design of Mining Machinery, Department of Mineral Resources Engineering, University of Leoben, Austria.

[3]Senior Researcher, Department of Mineral Resources Engineering, University of Leoben, Austria.

Abstract. The following paper is discussing the predictability of the cutting force of small, longitudinal part-face cutter heads in soft rock conditions. This includes a review of theoretical rock cutting models for estimating the cutting force of conical pick tools, experimental tests of a small, longitudinal part-face cutter head and assessing the applicability of single-pick rock cutting models to full-scale cutting operations. Experimental cutting tests with three different rock strengths (UCS = 16, 23 and 30 MPa) have been conducted successfully and the obtained results were taken to develop a sophisticated approach to predict the cutting forces with an empirical-numerical approach. Due to the comparatively small dimensions of the conical pick tools, major deviations between the single-pick cutting force models and measurement results could be found. This limitation necessitated the introduction of a scale factor to accurately predict the cutting force of single picks in contact. With the adapted model it is possible to calculate the maximum cutting force of a single pick cutting with only minor deviations. Scaling up this approach to predict the cutting force and cutting torque for a full-scale cutter head is only possible by neglecting the effect of the variable cutting depth during the cutting operation. Therefore, a new model has been developed which is capable of including this effect in the cutting force prediction. With this new approach, the cutting operation of a longitudinal part-face cutter head can be simulated and results showed a mean relative deviation of 4 % between the measured and simulated total cutting forces.

1 Introduction

The mining industry faces increasing challenges related to sustainability and ecological aspects that require additional efforts in research and development. A significant trend in underground mining is the movement towards zero personnel, which demands the full mechanization and subsequent automation of the mining process up to the use of fully autonomously operating robots [1, 2]. This intention aims to reduce the residual risk to a minimum for workers in harsh mining conditions [3]. Therefore, there is an urgent need to develop automated mining machines that can take over the hazardous parts of the mining operation. [4]

Currently, some mining operations are already done entirely by independently working machines, but there is still personnel required for various tasks, such as maintenance and surveillance. To overcome this challenge, there is a need to develop robots that can perform maintenance tasks on mining machines (semi-)autonomously [5]. Furthermore, the use of robots for exploration of abandoned mines and selective mining, especially

in difficult to access areas, is also a potential area for research and development in the upcoming years. [3, 6]

Future mining robots neither belong to the class of classical robots nor to industrial mining machines. Mobile robots have a much lower mass (usually < 100 kg) [7], while mining machines typically have masses beyond 10 t up to over 100 t due to their performance orientation. The classification of robot types and industrial mining machinery is presented in Figure 1.

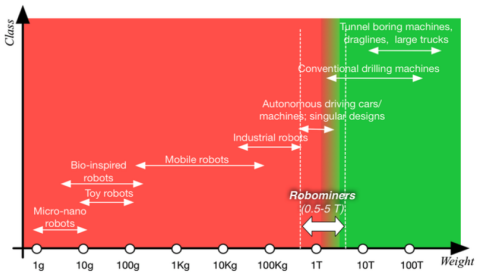

Figure 1: Robotics in mining - Categories [8]

Small-scale mining robots need to be equipped with a suitable excavation tool to create tunnels or excavate ore. Excavation systems can either be mechanical, alternative or combined excavation systems. In hard rock scenarios, drill and blast is up to this date most likely the only potential excavation method with a decent efficiency for small mining robots [4]. Although mechanical excavation methods are limited and highly depending on power and machine mass, they have the advantage of a continuous excavation process [9]. Alternative excavation methods are not based on a mechanical tool-rock interaction and the much smaller reaction forces are enabling the ability of mining harder rock. The downside of excavation tools using an alternative energy source (e.g. high-pressure waterjet cutting or hydrofracturing) is the high specific energy [10].

In industrial mining, the economy of the mining process must be guaranteed in order to have a profitable operation. In a smaller scale and for non-profit research purposes, the energy required to excavate a unit volume of material can be much higher. That could be causing the employment of alternative excavation systems as sustainable and continuous tools in small-scale mining robots for special mining scenarios or exploration operations in the futures. [4, 11, 12]

Mechanical cutting systems are prominent tools in the mining and tunneling industry. Therefore, the scalability and potential of a small-scale production tool system for a robotic mining machine with comparatively low mass have been evaluated. This paper is resulting from an applicability assessment of a small-scale part-face cutter head as production tool unit for a prototype of a robotic miner. A major challenge state the high reaction forces which a machine is limited of handling. Hence, the prediction of the cutting forces is a key task in developing future excavation systems for small-scale machines. [11, 12]

In order to evaluate the efficiency of a small, longitudinal cutter head, a full-scale laboratory test rig has been developed. This test rig allows testing the cutting performance with various rock samples while measuring the forces acting on the system, including cutting torque and cutting force.

The measurements were compared to profound rock cutting theories and the conclusions have been taken to understand the scalability problem of single-pick rock cutting theories to a full-scale prediction model. Eventually, a model for predicting the cutting force of a longitudinal cutter head, which considers the changing cutting depth of the pick during the cutting process, has been developed.

2 Theoretical background on mechanical cutting

In this chapter, the theoretical background of mechanical cutting with focus on rock cutting with conical pick tools will be outlined. The standard mechanical cutting machines use cutting drums (like a continuous miner) or cutter heads (like a roadheader) to excavate ore. Cutter heads are typically either transversal or longitudinal cutter heads. Transversal cutter heads exhibit a general higher efficiency, are capable of cutting harder

rock compared to longitudinal cutter heads and therefore have become established as a prominent machine in mining and tunneling. [13]

In [14], the maximum manageable reaction forces of a 1500 kg robot have been analysed for various mechanical excavation systems. The result of this study was that mechanical cutting leads to traction problems even at very low rock strengths. Taking this limitation into account, it makes sense to use a longitudinal cutter head, as this ensures a reasonable cutting performance in this small scale. Further advantages are the simpler design, less complex integration into an existing system and roughly similar excavation rates as transversal cutter heads in soft rock conditions.

2.1 Longitudinal cutter head

A longitudinal cutter head has the rotation axis of the cutter head in-line with the boom axis (Figure 2). The picks are arranged in a spiral shape up to the front end of the drum [15]. The positions of the picks are precisely defined and have to be harmonized in order to generate a continuous excavation pattern without interfering with each other and to excavate the entire cutting volume while moving the boom. [13, 16]

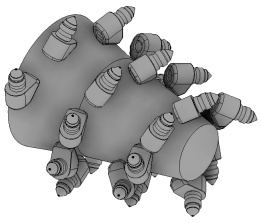

Figure 2: Longitudinal cutter head

The design of the cutter head is highly depending on the material to be excavated, taking into account various rock characteristics, the overall rock mass rating and carrier machine properties.

2.2 Conical pick tools

Roadheaders commonly use conical pick tools, which have a steel base body and a hardened steel tip. These rotationally symmetric tools usually feature a tungsten-carbide hard metal tip with cobalt as the binding material. The conical pick tool's shape and tip material quality can vary depending on the intended application. The pick tools are axially fixed inside a tool holder but are rotatable to enable a uniform wear profile. [15]

2.2.1 Pick forces

The resulting force acting on a pick can be separated in the cutting force F_c, the normal force F_n and the side force F_s. The cutting force is pointing in the direction of the pick's motion and is generally parallel to the cut surface. It is depending on the rock strength and responsible for chip formation in the rock mass. A threshold value needs to be exceeded to initiate cracks in the rock. The normal force points towards the cutter drum and is perpendicular to the cutting force. It is also known as passive force, because it is applying pressure on the pick and pushing the machine away from the rock face. Consequently, it is a function of the contact area between the tip of the pick and the cut surface. The side force acts on the side of the pick. This force occurs, because the picks are not installed perpendicular to the rotation axis. The occurring forces and the corresponding geometrical angles are shown in Figure 3. [17]

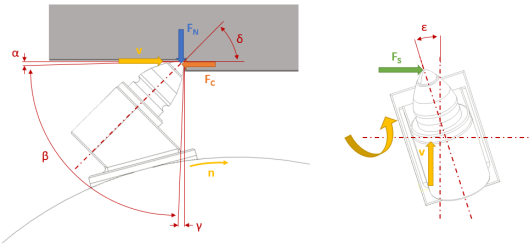

Figure 3: Conical pick tool - Forces and angles

The pick orientation is described by the clearance angle α, the rake angle γ, the attack angle δ and the tilt angle ϵ, whereas the geometry of the pick tip is defined by the tip angle β.

3 Cutter head test rig

In order to test the efficiency and performance of a small-scale, longitudinal cutter head, a suitable full-scale test rig has been developed. The cutter head is mounted on a linear guidance and powered by a hydraulic motor. A double-acting cylinder in the rear of the production tool assembly is moving the system axially and another cylinder is pushing or pulling the rock sample which is fixed inside a cage. The test samples can have a size of up to $400 \times 230 \times 300$ mm ($w \times l \times h$). The test rig with its components can be seen in Figure 4.

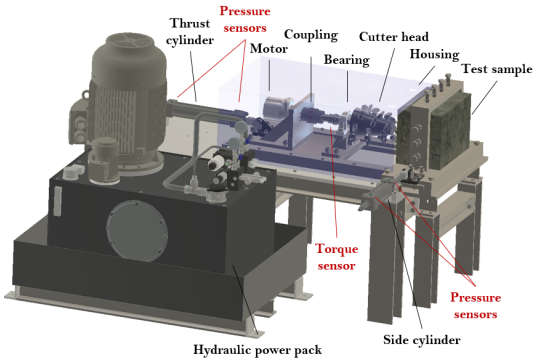

Figure 4: Cutter head test rig - CAD model

A detail of the test rig with focus on the cutter head, torque sensor and a partly-cut concrete sample is presented in Figure 5.

Figure 5: Cutter head test rig - Detail

3.1 Cutting tests

The performance of the cutter head has been tested by a predefined test cycle (see Figure 6) which is consisting of two cutting operations:

- Axial thrust: Sumping-in into the rock sample axially by actuating the thrust cylinder.
- Radial slew: Cutting the rock sample radially by actuating the side cylinder and moving the rock sample.

The rotational speed of the cutter head has been set at a constant speed of n = 300 rpm, whereas two slew speed levels (v_s = 7 mm/s and 14 mm/s) have been used. For each rock strength category, 5 test sets have been made to minimize statistical errors.

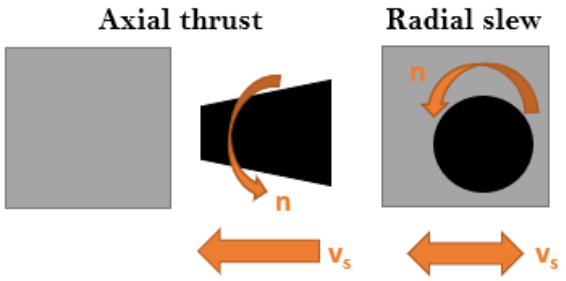

Figure 6: Test cycle

In each test, cylinder forces and cutting torque have been measured constantly. The cylinder force measurement was performed by pressure sensors and the data was processed in real-time with an Arduino microcontroller to be able to monitor them during the tests. Measuring the cutting torque was done by strain gauge assembly and processing equipment inside a 3D-printed housing which was mounted on the shaft of the cutter head. The cutting force was eventually derived from the cutting torque and the effective pick radius.
Three different rock strengths have been tested:

- B20 concrete: σ_c = 23 MPa.
- B30 concrete: σ_c = 30 MPa.
- Oilshale: σ_c = 16 MPa.

The oilshale samples were casted inside concrete to obtain a compact sample.

3.2 Results

The cutting forces of all test sets can be seen in Figure 7. It is clearly evident, that the cutting force increases with higher rock strenghts. Depending on the total sump-in depth of the cutter head, a slightly degressive increase of the cutting force can be recognized, although the number of picks in contact is increasing linearly. This is due to the fact, that the individual cutting forces of the picks are not constant throughout their respective contact time.

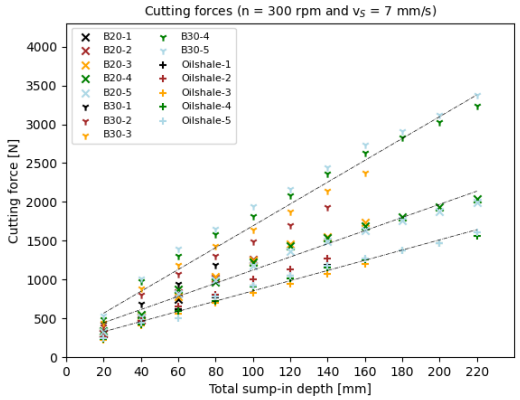

Figure 7: Measured cutting forces

As the cutting torque and cutting force are linearly related, the cutting torque shows the same behaviour as the cutting force (Figure 8).

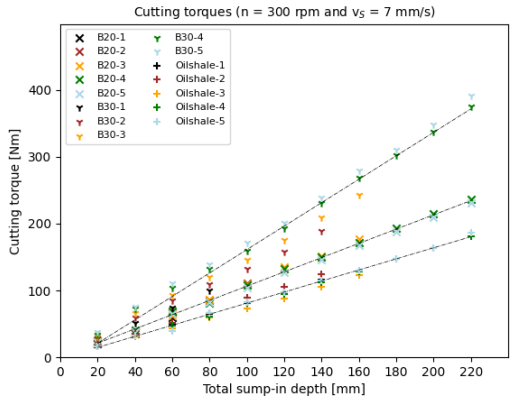

Figure 8: Measured cutting torques

The relation between the cutting force and the total sump-in depth respectively the cutter head position are described in more detail in chapter 5.

4 Simplified cutting force prediction model

Numerous single-pick cutting force estimation models have been developed over the last decades since the application of conical pick tools in mining has set in. In the following section, well known approaches have been analysed and compared to the experimental test data.

4.1 Cutting force models for conical picks tools

Yasar [18] extensively reviewed some rock cutting theories: Lundberg [19] conducted the initial study on rock cutting/indentation with conical picks, following their usage on mechanical cutting machines. It was found that the formation of radial cracks during indentation of conical picks occurs due to the rock's tensile strength being exceeded [19]. Evans [20] proposed the first theory on cutting rock with conical picks. As per Evans' theory, when a conical pick is forced to indent into rock, it generates a hole underneath it, accompanied by the formation of radial compressive stresses. Evans' theory also suggests the presence of tensile stresses accompanying the radial compressive stresses, which open up the crack interface [20]. [18]

Theory of Evans

Evans approach (Equation 1) is considering both the compressive strength σ_c and the tensile strength σ_t of the rock. The interaction between the pick and the rock is taken into account by the pick cutting depth d and the pick geometry is defined by the semi-cone angle θ (where, $\theta = \beta/2$). [20]

$$F_c = \frac{16\pi d^2 \sigma_t^2}{\sigma_c \cos^2 \theta} \tag{1}$$

[20]'s theory does not consider the effect of friction. Further on, the cutting force F_c is inversely proportional to the compressive strength σ_c and fails to attain a value of zero if the semi-cone angle θ reduces to zero. [18]

Theory of Roxborough
Additionally to Evans' theory, Roxborough [21] included the effect of friction in his approach (Equation 2). This friction coefficient is represented as angle ϕ. ϕ typically has a value between 10° and 30°. [18]

$$F_c = \frac{16\pi d^2 \sigma_c \sigma_t^2}{(2\sigma_t + \frac{\sigma_c \cos\theta}{1+\tan\phi/\tan\theta})^2} \tag{2}$$

Theory of Goktan
Goktan [22] stated a new hyptohesis (Equation 4.1) which is aiming to overcome the shortcomings of [20]'s theory.

$$F_c = \frac{4\pi d^2 \sigma_t \sin^2(\theta+\phi)}{\cos(\theta+\phi)} \tag{3}$$

None of the above mentioned theories considers the position of the pick relatively to the rock, which is usually described by the three pick angles but at least by one.

Theory of Goktan and Gunes
Goktan and Gunes [23] elaborated the approach by including the rake angle γ (Equation 4).

$$F_c = \frac{12\pi d^2 \sigma_t \sin^2[(90-\gamma)/(2+\phi)]}{[(90-\gamma)/(2+\phi)]} \tag{4}$$

To understand the behaviour of the individual theories, the single-pick cutting forces depending on the uniaxial compressive strength have been calculated and visualized (see Figure 9). It is important to note, that for calculation, the tensile strength σ_t was chosen to be 10 % of the compressive strength σ_c. A clearly linear behaviour can be seen, which matches with experimental data. [15, 18]

The pick cutting depth d has been set to 5 mm, the semi-cone angle θ to 80° for standard conical pick tools [23], the friction angle ϕ to 10° [23] and the rake angle γ of the pick to -7° [23].

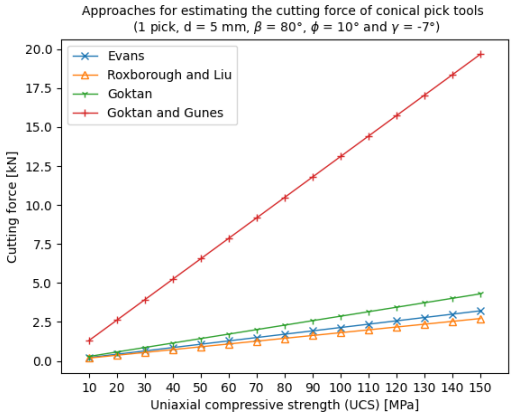

Figure 9: Comparison of cutting force estimation models

Interestingly, the theories of Evans, Roxborough and Goktan provide cutting forces of similar value, whereas the theory of Goktan and Gunes results in much higher magnitudes. This divergence is presented in Figure 10.

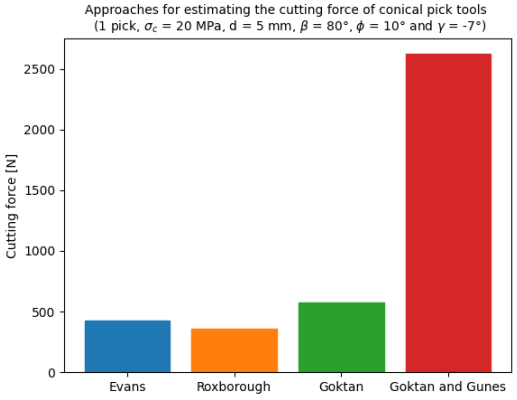

Figure 10: Comparison of cutting force estimation models - 1 pick and $\sigma_c = 20$ MPa

It should be noted that the only theory regarding true conical pick cutting is Evans' study from 1984. All other models are simply modifications of Evans' theory. However, Evans developed his theory based on the concept of indentation, which does not accurately reflect the actual cutting conditions observed in laboratory or field settings with conical picks. A theory focused on the mechanics of conical pick cutting should take into

account the cutting conditions more realistically. [18]

Eventually, if the cutting forces of experimental data is extracted for different rock strengths, processed and with the help of linear regression, the cutting force depending on the uniaxial compressive strength (UCS) can be predicted. Because the measurements only have been made with a maximum UCS of 30 MPa, the results are treated very cautiously, but the same linear behaviour can be observed (see Figure 11).

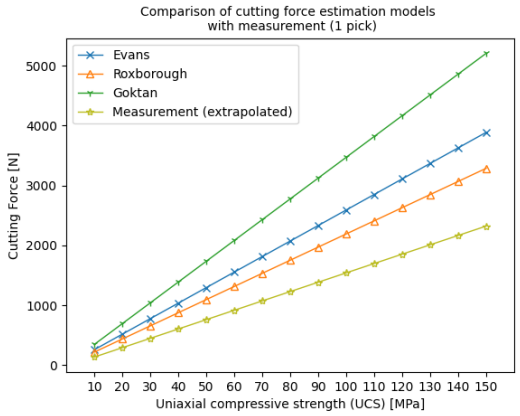

Figure 11: Comparison of cutting force estimation models with measurement depending on UCS

Quantifying the obtained results is done in the next section by comparing the calculated cutting forces with the experimental results.

4.2 Modified single-pick cutting force model

In Figure 12, the experimental data is compared with the obtained cutting forces from the individual rock cutting theories. Note: The cutting force resulting from the experimental data shows the maximum cutting force during a full pick contact cycle (180°). Due to the already very high resulting forces from the theory of [23], those results were omitted for further comparison.

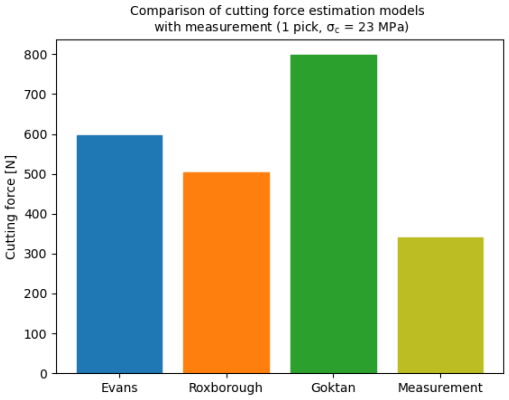

Figure 12: Comparison of cutting force estimation models with measurement - 1 pick

None of the calculated single-pick cutting forces show a similar magnitude as the measured cutting force, which are much higher than the cutting forces provided by the reviewed rock cutting theories. This might be attributable to the small-scale of the conical picks used in the experimental test. Although smaller picks have a significantly smaller contact area, which causes less friction, with the theories of [20, 21, 22] it is not possible to estimate the cutting forces for comparatively small cutting depths (< 5 mm).

Modified theory of Roxborough

Although, no hypothesis showed a good compliance with the experimental data, the formula of Roxborough is used and rearranged with an additional scale factor k to compensate the smaller pick dimensions (Equation 5). The factor k needs to be calibrated for every individual pick dimension and in this case it has been agreed on $k = 3.15$.

$$F_c = k^2 \cdot \frac{16\pi d^2 \sigma_c \sigma_t^2}{(2\sigma_t + \frac{\sigma_c \cos\theta}{1+\tan\phi/\tan\theta})^2} \tag{5}$$

Comparing the modified theory with more experimental data shows a very good agreement in soft rock conditions (see Figure 13).

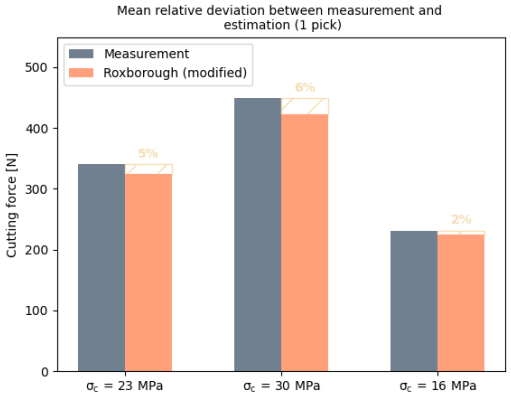

Figure 13: Comparison of modified Roxborough theory with measurement

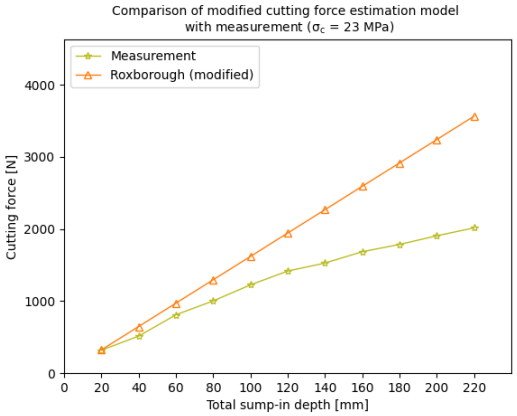

Figure 14: Full-scale comparison of modified Roxborough model with measurement

4.2.1 Limitations

The modified approach has some limitations: If the cutting models from the previous section are taken to calculate the total cutting force of a full-scale cutter head during a cutting operation, it is only possible by mutliplying the single cutting force with the number of picks in contact (Equation 6).

$$F_{c,total} = F_c(d_{max}) \cdot n \tag{6}$$

That approach leads to a linear behaviour between the total-sump in depth of the cutter head and the total cutting force $F_{c,total}$. However, in reality, the cutting force is a function of the cutting depth of the pick (Equation 7).

$$F_{c,total} = \sum_{n=1} F_{c,n}(d_{\theta,n}) \tag{7}$$

The cutting depth of a pick is not constant throughout a contact cycle. Depending on the relative position, the rotation direction and slewing direction of the cutter head, the cutting depth of the pick is either increasing (progressive cut), decreasing (degressive cut) or a combination (full cut). A detailed investigation on the behaviour of the cutting depth of a pick will be done in chapter 5. Figure 14 shows the theoretical cutting force of a cutter head depending on the total sump-in depth compared to the experimental data.

The theoretical results show a linear increase of the cutting force (Equation 6), whereby the experimental data clearly shows a degressive behaviour of the total cutting force $F_{c,total}$. This phenomena results because of the overlapping contact paths of the individual picks.

5 Cutter head simulation model

Within this work, a kinematic model of the pick cutting process has been developed to analyse the influence of the changing depth of the pick on the cutting force. The simulation includes the modelling of the entire cutter head system with the specified pick positions (Figure 15).

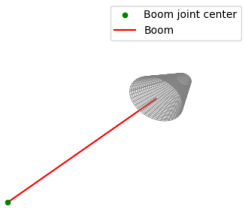

Figure 15: Longitudinal cutter head model

5.1 Configuration

The longitudinal cutter head is modelled with its external dimensions and pick positions. Same as to the cutter head used in the experimental tests (see Figure 16), 24 picks are placed onto the surface of the cutter head, whereas they appear in pairs on 180° offset spirals.

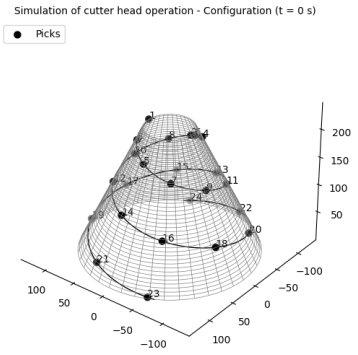

Figure 16: Simulation of cutting process - Configuration of cutter head

The interaction between the cutter head with the rock can be distinguished in three contact types. The cutting depth of the pick changes with the rotation angle of the cutter head.

- Progressive cut: the cutting depth is increasing from a minimum (~ 0) to a maximum.
- Degressive cut: the cutting depth is decreasing from a maximum to a minimum.
- Full contact cut: A combination of progressive and degressive cut.

The experimental setup was mainly focusing on the full contact cut case. Each individual pick is in contact with the rock for 180°. Figure 17 shows the contact angles of the picks on the cutter head.

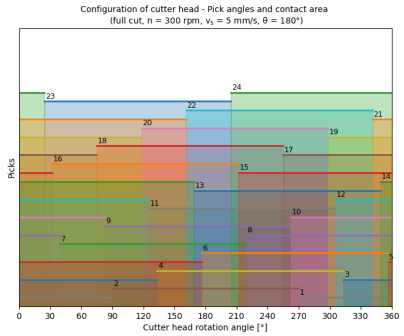

Figure 17: Simulation of cutting process - Configuration of pick contact angles

The pick contact angles will further be used to define start and end time of a single pick's contact.

5.2 Consideration of the changing pick cutting depth

The pick cutting depth is a function of the rotation angle and the slew speed ($d = f(\theta, v_s)$). The pick kinematics are modelled with Equation 8.

$$p(t) : \begin{cases} x(t) = r \cdot \cos\theta + v_s \cdot t \\ y(t) = r \cdot \sin\theta \end{cases} \tag{8}$$

Where r defines the effective pick radius, θ the rotation angle and v_s the slew speed. The pick cutting depth d_θ is calculated according to Equation 9.

$$d_\theta = \sqrt{(x(t) - x_0)^2 + (y(t) - y_0)^2} \tag{9}$$

The cutting force F_c is calculated with the modified cutting force model, described in section 4.2 and combined with the above equations incorporates a dynamic behavior ($F_c = f(\theta, v_s)$). The total cutting force $F_{c,total}$ of the cutter head is obtained by Equation 10, where n is the number of picks in contact.

$$F_{c,total} = \sum_{n=1} F_{c,n}(d_{\theta,n}) \tag{10}$$

Equation 11 describes the calculation of the total cutting torque $T_{c,total}$.

$$T_{c,total} = \sum_{n=1} F_{c,n}(d_{\theta,n}) \cdot r_{eff,n} \tag{11}$$

Where r_{eff} is the effective pick radius.

5.2.1 Cutting depth

In Figure 18, a simplified model of three picks in contact is seen, in which the picks have an individual offset of 20°. The paths of the picks over the rotation angle are visualized and the profile of a full cut operation can be recognized on the basis of the pick cutting depth courses.

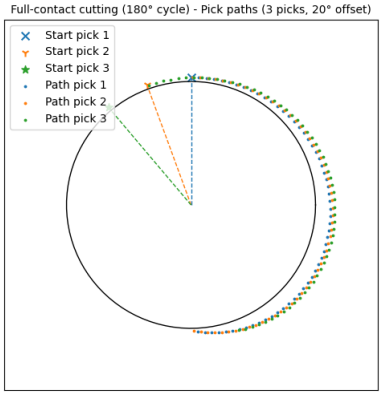

Figure 18: Full cut - Illustration of pick paths with horizontal slew

According to Equation 9, the individual cutting depths are calculated and plotted over the rotation angle. A shift of the cutting depth maximum by 20° can be seen in Figure 19.

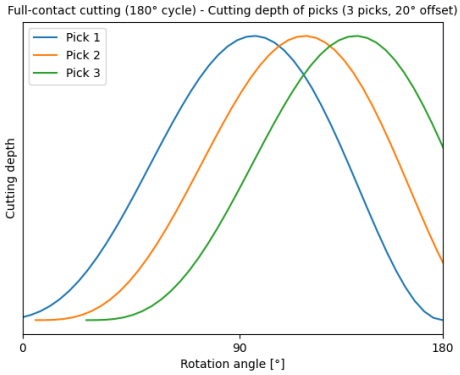

Figure 19: Cutting depths depending on rotation angles of pick

For longitudinal cutter heads, the maximum cutting depth d_{max} of a single pick is defined by the interaction of the rotational speed and slew speed.

The pick cutting depth progressions of the modelled cutter head are visualized in Figure 20.

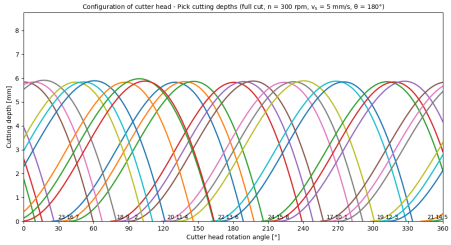

Figure 20: Pick cutting depths depending on rotation angle of cutter head

An even distribution of the picks along the cutter head's circumference can be found.

5.2.2 Cutting force

Once the single-pick cutting depths are determined, the cutting force can be computed with Equation 12.

$$F_c = k^2 \cdot \frac{16\pi d_\theta^2 \sigma_c \sigma_t^2}{(2\sigma_t + \frac{\sigma_c \cos\theta}{1+\tan\phi/\tan\theta})^2} \qquad (12)$$

The exemplary cutting forces of the three-picks-model with the total cutting force $F_{c,total}$ are presented in Figure 21.

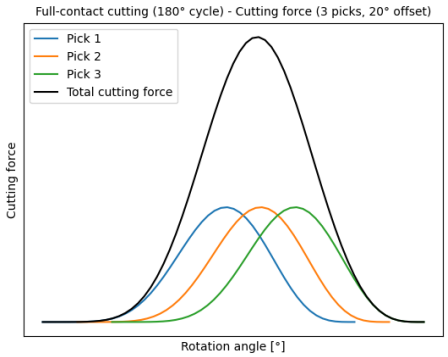

Figure 21: Cutting forces depending on rotation angles of pick

Hereby, the issue mentioned in section 4.2.1 is overcome due to the dynamic characteristic of the cutting depth. In summary, the total cutting force $F_{c,total}$ is not a linear multiple of the individual forces. Instead, $F_{c,total}$ is less than the value predicted with the upscaled single-pick theories. According to this information, the phenomena of the degressive behaviour of the total cutting force determined in experimental tests can be verified.

6 Validation

The developed simulation model in chapter 5 was validated with the data acquired in the experimental tests, which are discussed in section 3.2. Validating the model required a processing of the measurement data and is hereafter discussed for the B20 concrete cutting tests. Further validation has been performed for B30 concrete and Oilshale tests, each with slew speed $v_s = 7$ mm/s and 14 mm/s.

6.1 Objective

The aim of the subsequent process is the validation of the developed methodology for the simulation of the nonlinear total cutting force of a longitudinal cutter head as the experimental tests have shown.

6.2 B20 concrete cutting tests

To verify and validate the cutting force model, a trial of cutting tests was conducted. In these cutting tests, already described in section 3.1, test samples have been cut in a cyclical process. Predefined total sump-in depth levels have been established and the total sump-in depth for each test has been controlled by the axial thrust. For each level, the maximum cutting torque $T_{c,total}$ has been measured and the total cutting force $F_{c,total}$ has been derived from it (Figure 22).

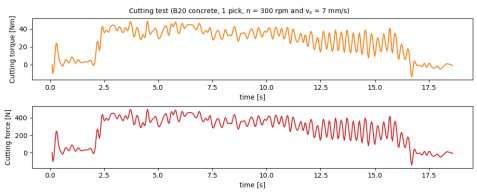

Figure 22: Exemplary measurements of cutting test

The comparison of cutting test and simulation is shown in Figure 23. The total cutting force is displayed for specified total sump-in depth levels. The arithmetic average total cutting forces of the maximum measured forces from 5 cutting tests are depicted and opposed with the simulation results.

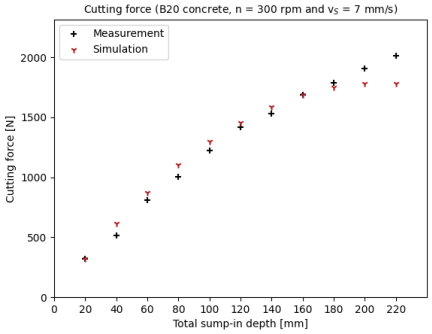

Figure 23: B20 concrete - Cutting force depending on total sump-in depth of cutter head

The comparison shows satisfying agreement between experimental data. Especially, the non-linear increase of the total cutting force could be simulated in a realistic behavior. Another comparison is done for the total cutting force as a function of number of picks in contact (see Figure 24).

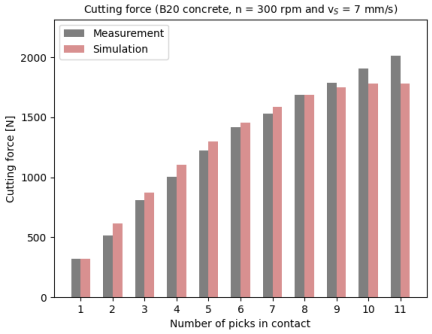

Figure 24: B20 concrete - Cutting force depending on number of picks in contact

Again, the simulation shows the same trend as the experimentally obtained data. The absolute deviations are marginal and overall, the simulation shows highly satisfactory results.

In Figure 25, the mean relative deviations between measurement and simulation are shown for the three test sample types.

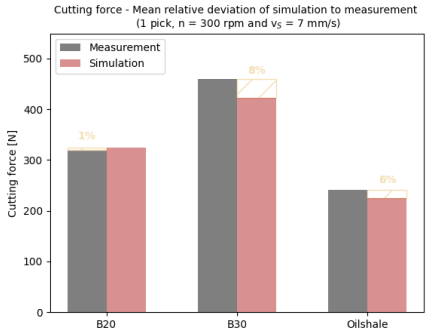

Figure 25: Cutting force for different test sample types

A maximum mean relative deviation of 7 % for the B20 concrete sample could be found, whereas the minimum mean relative deviation between measurement and simulation is 1 % for the Oilshale sample.

A linear regression of the measured cutting forces provides the trend of the cutting force as a function of the uniaxial compressive strength of the material. The graph is shown in Figure 26.

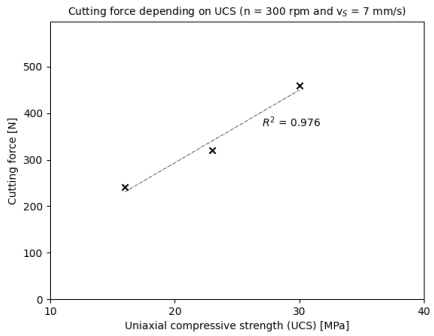

Figure 26: Measured cutting forces (1 pick) of test samples

The linear regression analysis yields a satisfactory coefficient of determination and can be summarized with Equation 13.

$$F_c(\sigma_c) = 15.6 \cdot \sigma_c - 19.0 \tag{13}$$

This equation can be exploited to show the trend also for higher uniaxial compressive strength regions. Compared with the cutting forces calculated with the modified single-pick cutting theory, the extrapolated data shows again good conformity (see Figure 27).

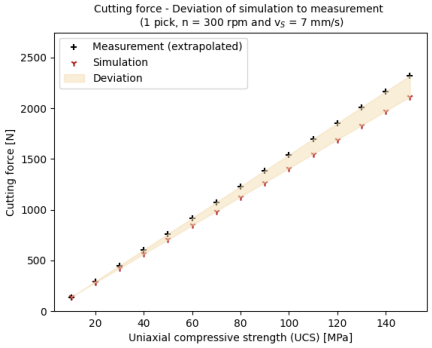

Figure 27: Cutting force depending on UCS - Measurement vs. simulation

Although it is important to mention, that the cutting forces above the maximum uniaxial compressive strength of the test sample types, need to be treated with caution. The relative deviations between extrapolated data and simulation are presented in Figure 28.

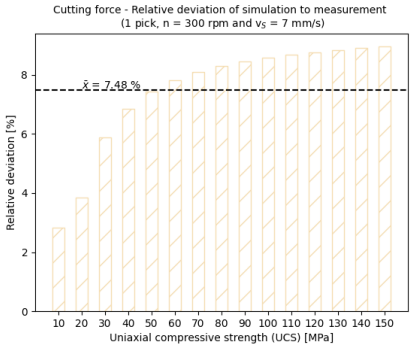

Figure 28: Relative deviations between simulated and measured cutting forces

The relative deviations provide pleasant results for uniaxial compressive strengths between 20 and 60 MPa, whereas above the threshold, the magnitudes are still decent. Solely for very soft rock material (< 20 MPa), the relative deviations exceed the average value by a factor of 2.

7 Conclusion

In conclusion, this study focused on the investigation of the cutting forces of a longitudinal cutter head through a series of experimental tests and the development of a simulation model. A review of existing, theoretical approaches for calculating the single-pick cutting force was conducted, and the best fitting theory was adapted for small-scale conical pick tools in this study. Additionally, a new simulation model was developed, which demonstrated a highly satisfactory degree of agreement with the experimental data.

The experimental tests conducted in this study provided valuable insights into the behavior of the cutting force under various rock strength conditions. Through these tests, the single-pick cutting force was determined and used to validate the simulation model. The use of both experimental and simulation methods enabled a comprehensive understanding of the cutting process, providing a more accurate and reliable methodology of predicting the total cutting force.

By reviewing existing rock cutting theories for calculating the single-pick cutting force, the upsides and limitations of each method have been highlighted. By adapting the model of Roxborough [21], it was possible to develop a more robust and accurate approach to predict the cutting force for small-scale conical picks.

The developed new simulation model allows a precise simulation of the cutter head and pick kinematics, particularly by considering the variable cutting depth of the pick.

A combination of the adapted method and the newly developed simulation model provided a simulation methodology for predicting the total cutting force of longitudinal cutter heads in various cutting conditions.

Funding

This project has received funding from the European Union's Horizon2020 research and innovation programme under grant agreement No. 820971.

References

[1] J. A. Marshall et al. "Robotics in Mining". In: *Springer Handbook of Robotics*. Ed. by Bruno Siciliano and Oussama Khatib. Cham: Springer International Publishing, 2016, pp. 1549–1576. ISBN: 978-3-319-32550-7.

[2] R. Hiltz. *Taking a step into the robotic future*. 2020. URL: https://www.miningmagazine.com/innovation/news/1387411/taking-step-into-the-robotic-future.

[3] N. A. Sifferlinger. "Roboter im Bergbau – wo liegt der Bedarf?" In: *BHM Berg- und Hüttenmännische Monatshefte* 166.2 (2021), pp. 53–58. ISSN: 0005-8912. DOI: 10.1007/s00501-021-01079-1.

[4] M. Berner and N. A. Sifferlinger. "Analysis of Excavation Methods for a Small-scale Mining Robot". In: *ISARC Proceedings* (2020).

[5] A. Chakravorty. "Underground Robots: How Robotics Is Changing the Mining Industry". In: *Eos* 100 (2019). ISSN: 2324-9250. DOI: 10.1029/2019EO121687.

[6] M. Berner and N. A. Sifferlinger. "H2020 – ROBOMINERS". In: *BHM Berg- und Hüttenmännische Monatshefte* 166.2 (2021), pp. 59–63. ISSN: 0005-8912. DOI: 10.1007/s00501-020-01074-y.

[7] B. Siciliano and O. Khatib, eds. *Springer Handbook of Robotics*. Cham: Springer International Publishing, 2016. ISBN: 978-3-319-32550-7. DOI: 10.1007/978-3-319-32552-1.

[8] European Commission. *ROBOMINERS Proposal SEP-210520664: Resilient Bio-inspired Modular Robotic Miners / ROBOMINERS*. Ed. by European Commission. 2018.

[9] N. A. Sifferlinger. "Stand der mechanischen Löseverfahren im Bergbau". In: *BHM Berg- und Hüttenmännische Monatshefte* 167.2 (2022), pp. 43–51. ISSN: 0005-8912. DOI: 10.1007/s00501-022-01195-6.

[10] M. Berner and N. A. Sifferlinger. "Need of Alternative Excavation Tools for Mining Robots". In: *Proceedings of the 18th International Conference on Mineral Processing and Geometallurgy*. Vol. 18. 2022, pp. 270–281.

[11] M. Berner and N. A. Sifferlinger. "Abbautechnologien für zukünftige, mobile Bergbau-Roboter". In: *BHM Berg- und Hüttenmännische Monatshefte* 167.2 (2022), pp. 76–83. ISSN: 0005-8912. DOI: 10.1007/s00501-022-01194-7.

[12] N. A. Sifferlinger, P. Hartlieb, and P. Moser. "The Importance of Research on Alternative and Hybrid Rock Extraction Methods". In: *BHM Berg- und Hüttenmännische Monatshefte* 162.2 (2017), pp. 58–66. ISSN: 0005-8912. DOI: 10.1007/s00501-017-0574-y.

[13] M. Berner, N. A. Sifferlinger, and R. Narimani Dehnavi. *ROBOMINERS DELIVERABLE D6.4: PRODUCTION TOOLS CONCEPTUALIZATION AND RESEARCH AT TRL-3*. Ed. by ROBOMINERS Consortium. 2022.

[14] M. Berner and N. A. Sifferlinger. "Status of the H2020-ROBOMINERS Prototype". In: *BHM Berg- und Hüttenmännische Monatshefte* 168.2 (Feb. 2023), pp. 45–55. DOI: 10.1007/s00501-023-01318-7.

[15] N. Bilgin, H. Copur, and C. Balci. *Mechanical Excavation in Mining and Civil Industries*. Hoboken: Taylor and Francis, 2013. ISBN: 978-1-4665-8475-4.

[16] M. Berner, N. A. Sifferlinger, and R. Gerer. *ROBOMINERS DELIVERABLE D6.5: DEVELOP A SMALL-SCALE EXCAVATION TOOL SYSTEM FOR THE SELECTIVE MINING DEMONSTRATOR BASED ON COTS*. Ed. by ROBOMINERS Consortium. 2022.

[17] N. A. Sifferlinger. *Excavation Engineering - Mechanical Excavation*. Ed. by Lehrstuhl für Bergbaukunde, Bergtechnik und Bergwirtschaft. Leoben, 2022.

[18] S. Yasar and A. O. Yilmaz. "Drag pick cutting tests: A comparison between experimental and theoretical results". In: *Journal of Rock Mechanics and Geotechnical Engineering* 10.5 (2018), pp. 893–906. ISSN: 1674-7755. DOI: https://doi.org/10.1016/j.jrmge.2018.02.007.

[19] B. Lundberg. "Penetration of rock by conical indenters". In: *International Journal of Rock Mechanics and Mining Sciences Geomechanics Abstracts* 11.6 (1974), pp. 209–214. ISSN: 0148-9062. DOI: https://doi.org/10.1016/0148-9062(74)90127-2.

[20] I. Evans. "A theory of the cutting force for point-attack picks". In: *International Journal of Mining Engineering* 2.1 (1984), pp. 63–71. ISSN: 0263-4546. DOI: 10.1007/BF00880858.

[21] F. F. Roxborough and Z. C. Liu. "Theoretical considerations on pick shape in rock and coal cutting". In: *Proceedings of the Sixth Underground Operator's Conference* (1995), pp. 189–193.

[22] R. M. Goktan. "A suggested improvement on Evans's cutting theory for conical bits". In: *Proceedings of the Fourth International Symposium on Mine Mechanization and Automation* 1 (1997), pp. 57–61.

[23] R. M. Goktan and N. Gunes. "A semi-empirical approach to cutting force prediction for point-attack picks". In: *Journal of the South African Institute of Mining and Metallurgy* 105.4 (2005), pp. 257–263.